

## Preparation of activated carbon from oil palm fruit bunch for the adsorption of Acid Red 1 using optimized Response surface methodology

Manase Auta<sup>1</sup>, \*Mohammed Jibril<sup>2,3</sup>, Philip B.L. Tamuno<sup>4</sup>, Aboje Alechenu Audu<sup>1</sup>

<sup>1</sup>Federal University of Technology, Department of Chemical Engineering, P.M.B. 65, Minna, Nigeria

<sup>2</sup>Department of Chemical Engineering, Universiti Teknologi Malaysia, 81310 Skudai, Johor, Malaysia.

<sup>3</sup>Chemical Engineering Programme, Abubakar Tafawa Balewa University, Bauchi, P. M. B. 0248, Bauchi-Nigeria.

<sup>4</sup>Estates, Commercial Directorate, East Sussex Healthcare NHS Trust, Kings Drive, Eastbourne, BN21 2UD, United Kingdom.

### Abstract

Oil palm empty fruit bunch (OPEFB); a renewable agricultural waste material's potential was harnessed for adsorption of Acid Red 1 (AR1). Potassium hydroxide was impregnated on the precursor (OPEFB) for the production of activated carbon through chemical activation method under inert atmosphere of nitrogen. Activation temperature, chemical impregnation ratio (KOH:char) IR, and activation time were the preparation conditions investigated in this study. Central composite design (CDD) was used to develop two models which were used for determination of effects of selected conditions of preparation of OPEFB activated carbon yield and its performance in adsorbing AR1. Adsorption capacity of 197.62 mg/g (98.81%) and 19.12% yield were obtained at activation temperature of 820 °C, IR 2.5 and 140 min. There was good correlation between the experimental results and the predicted models obtained. The Brunauer Emmett Teller (BET) analysis of the activated carbon prepared at optimum conditions had a surface area of 820 m<sup>2</sup>/g, total pore volume of 0.52 cm<sup>3</sup>/g and scanning electron microscopy SEM was carried out to determine its surface morphology that enhance adsorption of AR1 on OPEFB activated carbon.

*Keywords:* Adsorption, Central composite design, Chemical activation, Optimization.

### 1. Introduction

The versatility of dye usage in many industries such as cosmetics, pulp and paper, textiles, electroplating, just to mention a few has exponentially increased its pollution to the environment due to non-compliance of the user industries to environmental laws. Above 10% of the estimated 10,000 dye types are used for dyeing in textile industries [1]; and about 146,000 tons from approximately 700,000 tons produced annually, are discharged along with waste water thereby polluting the environment [2]. The diverse nature of dye constituents (surfactants, organic products, inorganic polymers, biodegradability, acids and alkalis) makes them dangerous when released to the environment [3]. The negative effect of dye pollution includes retardation of photosynthesis activities, impeding light penetration, suppression of immune system of living things, making them susceptible to cancer, diarrhea, epidermis infection, leukemia and so on [4]. Efforts made to regulate this has either been neglected or costly to maintain by defaulters [5,6].

Adsorption approach is outstandingly efficacious and cost effective when compared with other methods like electrochemical coagulation, photochemical treatment, and membrane system etc [7]. Finding alternatives to the overpriced commercial activated carbon has been the focus of researchers towards promoting the use of adsorption process to tackle evacuation of dye from waste waters [8].

This challenge has prompted research into finding alternative or substitutes to the expensive commercial activated carbons by exploring other sources of raw materials for its production. Eco-friendly, cheaper and renewable agricultural raw materials have been found to be promising raw materials that can replace more expensive coal for production of qualitative and effective activated carbon. In literature, activated carbon has been produced from coconut husk, coconut shell, rice husk, corncobs, bamboo, saw dust, waste tea. [9,10].

Palm trees entirely are a good source of activated carbons [11,12]; but to the best of our knowledge, there is no report on the production of activated carbon from oil palm empty fruit bunch (OPEFB) for adsorption of Acid Red 1 dye (AR1). Therefore, this research is aimed at optimizing preparation parameters for production of activated carbon from oil palm empty fruit bunch for adsorption of AR1. Potassium hydroxide was chosen as activation agent because of its efficiency and effectiveness in developing different types of pores and high

surface areas on carbonaceous materials [13]. Some of the most important preparation conditions: activation temperature, chemical impregnation ratio IR and activation time [4] were optimized using response surface methodology RSM, an experimental design technique which is a useful tool in studying interactions between two or more variables.

## 2. Materials and methods

### 2.1 Materials

All chemicals were purchased from Merck Company and Sigma-Aldrich companies and used without further purifications. Acid Red 1 dye has chemical formula of  $C_{18}H_{13}N_3Na_2O_8S_2$ , colour index number 18050 and a molecular weight of 509.42; the structure of the dye is shown in Fig. 1. The empty fruit bunches were obtained from Enugu oil palm processing site in Nigeria. The precursor was pretreated by washing thoroughly with distilled water, dried in the oven at  $110\text{ }^{\circ}\text{C}$  for 6 h, grounded and sieved to 300-500  $\mu\text{m}$  sizes and packed for use.

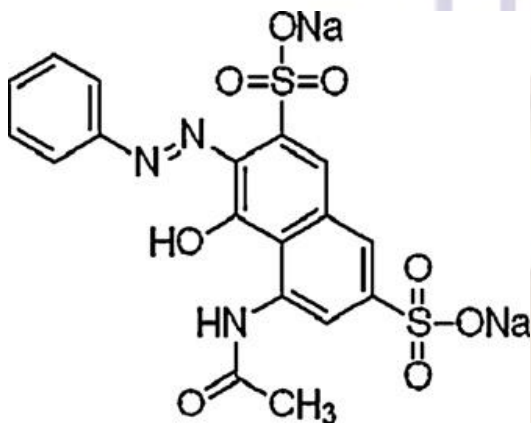


Figure. 1 Structure of Acid Red 1

### 2.2 Preparation of activated carbon

The pretreated OPEFB was carbonized in a furnace set at  $700\text{ }^{\circ}\text{C}$ , heating rate of  $5\text{ }^{\circ}\text{C}/\text{min}$  for 2 h in an inert nitrogen flow ( $100\text{ cm}^3/\text{min}$ ) atmosphere. A  $2^3$  full factorial experimental design was used to prepare the carbon for subsequent activation with ranges of: activation temperature  $500\text{--}800\text{ }^{\circ}\text{C}$ , chemical impregnation ratio of 0.3-2.5, and activation time ranging from 60-150 min. A ratio of potassium hydroxide to precursor (0.3:1-2.5:1) was impregnated and the mixture was kept overnight then dehydrated in the oven at  $110\text{ }^{\circ}\text{C}$  before activation under conditions similar to that of carbonization process as determined by the factorial design. The resulting activated carbon was washed thoroughly with distilled water to pH of 6.8-7, dried in the oven for 6 h and then packed in air tight container for use.

### 2.3 Activated carbon yield

The prepared OPEFB yield was calculated as:

$$\text{Yield (\%)} = \frac{\text{weight (g) of OPEFB produced}}{\text{weight (g) dried OPEFB carbon used}} \quad 1$$

### 2.4 Characterization of OPEFB activated carbon

The OPEFB activated carbon prepared at the optimum optimized conditions had its surface area, pore volume and average pore diameter determined using Micrometrics ASAP 2020 volumetric adsorption analyzer. Prior to analysis, the sample was degassed for 2 h under vacuum at  $300\text{ }^{\circ}\text{C}$ . After degassing, the sample was transferred to the analysis system where it was cooled in liquid nitrogen. A 21-point analysis was carried out at 77K to obtain the nitrogen adsorption-desorption isotherm by admitting successive known volumes of nitrogen in and out of the sample and measuring the equilibrium pressure. Brunauer-Emmett-Teller (BET) equation was used to determine the surface area of the sample and micro-pore volume was calculated using t-plot method.

The scanning electron microscopy (SEM) to determine Surface morphology of the sample was carried out using SEM analyzer JEOL, JSM-6460 LV, Japan.

### 2.5 Batch equilibrium studies

A set of 20 Erlenmeyer flasks of 250 mL representing the total number of experiments from the factorial design table were used for the studies. To each flask, 200 mL of 200 mg/L AR 1 dye solution and 0.2 g of OPEFB activated carbon was added and then placed in a water bath shaker at 30 °C with agitation speed of 130 rpm. The dye solution was maintained at its natural pH and allowed in the shaker until equilibrium was attained. Samples from each flask were collected, filtered and the residual concentration of the dye in the solution was determined at maximum wavelength of 530 nm with the aid of UV-Vis spectrophotometer. At equilibrium, the concentration of AR1 adsorbed was calculated using this equation:

$$Q_e = \frac{(C_o - C_e)V}{W} \quad 2$$

Where  $C_o$  and  $C_e$  (mg/L) are the initial and equilibrium concentration of the dye,  $V$  is the volume of the dye solution (mL) and  $W$  is the mass of the OPEFB adsorbent (g) used.

### 2.6 Design of experiment

A unit-factor approach method of optimizing preparation conditions of activated carbon is often cumbersome, uneconomical and has limitations for determining interaction effects of parameters amongst themselves. Therefore, a need for a tool that will integrate the factors (at certain operating specifications) simultaneously in relation to the expected responses set, to allow researchers' adequate understanding of the mechanism of the process is required. A mathematical statistical tool for design of experiment which enhances evaluation of simultaneous effects of operating parameters through formulation of models at optimal conditions used to predict the set responses called the Response surface methodology RSM was employed. It has been used to develop new processes, evaluate and optimize design parameters, and to develop new products. It has also been used in sorption processes to reduce process variability, improve on product yield, to reduce cost of development and to check correlation between raw materials and products [15]. One of the most popular RSM full factorial design known as central composite design CCD consisting of  $2^3$  runs,  $2(n)$  axial runs and six center runs ( $n$  is the number of factors) was used. In this study, a total of 20 experiments in accordance with the CCD full factorial which consisted of 8 factorial points, 6 axial points and 6 replicates at the center. The factorial points were notated as  $\pm 1$  giving rise to  $(\pm\alpha, 0, 0)$ ,  $(0, \pm\alpha, 0)$ ,  $(0, 0, \pm\alpha)$  axial points. The ability to rotate  $\alpha$ , depends on the number of points in the factorial portion of the design. It can be calculated as follows:

$$\alpha = (P)^{0.25} \quad 3$$

where  $P$  is the number of points in the cube portion of the design ( $P = 2^k$ ,  $k$  is the number of factors). To minimize the effect of uncontrolled factors, the experimental sequence was randomized. For this study, consideration of three factors will yield  $\alpha$  ( $2^3$ )<sup>0.25</sup> of 1.682. The parameters optimized were activation temperature  $x_1$ , activation time  $x_2$  and chemical impregnation ratio  $x_3$ . These three parameters together with their respective ranges were chosen based on the literature and preliminary studies as given in Table 1. A second degree order polynomial to develop empirical model that simultaneously correlates the parameters and the targeted response which is expressed as:

$$Y = b_o + \sum_{i=1}^n b_{ii}x_i + \left( \sum_{i=1}^n b_{ii}x_i \right)^2 + \sum_{i=1}^{n-1} \sum_{j=i+1}^n b_{ij}x_i x_j \quad 4$$

where  $Y$  is the predicted response,  $b_o$  is the constant coefficients,  $b_{ii}$  the quadratic coefficients,  $b_{ij}$  the interaction coefficients and  $x_i, x_j$  are the coded values of the variables considered. Model fitting and statistical analysis of the resulting model was done using Design Expert software version 6.0.6 (STAT-EASE Inc., Minneapolis, USA).

**Table 1** Coded levels for central composite design of independent variables

Variables (factors)	Code	Unit	Coded variable levels				
			$-\alpha$	-1	0	+1	$+\alpha$
Activation temperature	$x_1$	°C	650	690.54	750	809.45	850
Activation time	$x_2$	Min	60	84.32	120	155.68	180
Impregnation ratio (IR)	$x_3$	-	0.5	0.91	1.5	2.09	2.50

### 3. Results and discussion

#### 3.1 Characterization of OPEFB adsorbent

The summary of the BET surface analysis is summarized in Table 2 and the morphological structure of OPEFB and OPEFB activated carbon generated by SEM are shown in Fig. 2. The optimized OPEFB activated carbon produced had a very large surface area and was mesoporous (2.56 nm). The intensity of the pore opening can be seen in Fig. 2 which compared the precursor surface structure with the activated carbon produced from the OPEFB.

Table 2 Brunauer–Emmett–Teller analysis of OPEFB activated carbon

$S_{BET}$ ( $m^2/g$ )	$S_{ext}$ ( $m^2/g$ )	$S_{ext}/S_{BET}$ (%)	$S_{mic}$ ( $m^2/g$ )	$S_{mic}/S_{BET}$ (%)	$V_{tot}$ ( $cm^3/g$ )	$V_{mic}$ ( $cm^3/g$ )	$V_{mic}/V_{tot}$ (%)	$D_p$ (nm)
820.0	238.71	29.11	533.24	65.03	0.52	0.299	57.50	2.56

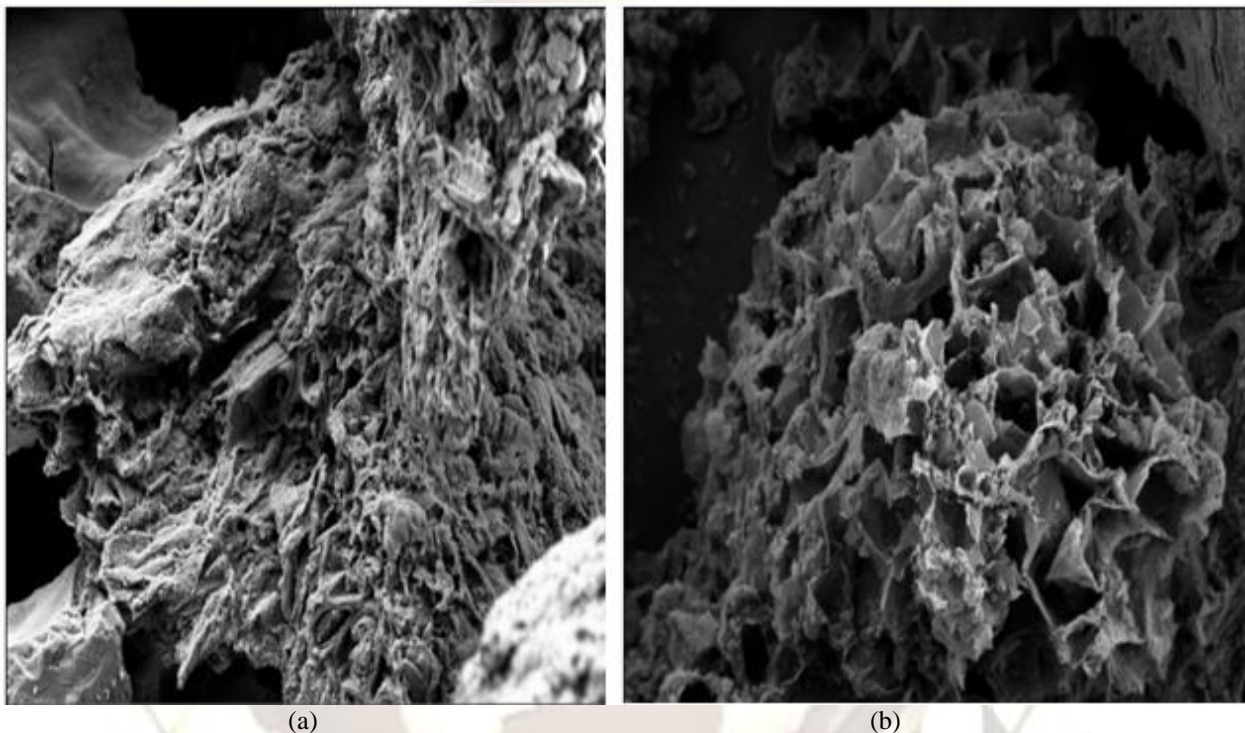


Figure 2 The SEM of (a) OPEFB precursor and (b) OPEFB activated carbon

#### 3.2 The optimization of yield and adsorption conditions

The responses yield and percentage removal of AR1 obtained due to effects of the parameters studied were evaluated using CCD design of experiment. The CCD was used in order to find the correlation between the parameters and the responses through some of its features such as the center points (run 15-20) used to determine the experimental error and the reproducibility of the data and the axial points for rotation. The complete experimental design with their responses is presented in Table 3. Quadratic models were suggested for the two responses percentage yield ( $Y_1$ ) and removal ( $Y_2$ ). The selected models were based on the highest sequential order polynomials according to the sequential sum of squares where the models were not aliased and the additional terms significant. The validity of the models was further ascertain by their correlation coefficient, standard deviation and adjusted R-squared values which were 0.92, 2.21, 0.86 and 0.94, 4.49, 0.89 for percentage yield and removal, respectively. The errors from the difference between the predicted and experimental data for yield and percentage removal of AR1 were 2.05 and 1.98, respectively; the results are summarized in Table 4. The range of results for the OPEFB activated carbon yield was between 7.9 to 25.53 % and 45.98 to 93.57 % for percentage removal of AR1 with the OPEFB respectively. The high values of  $R^2$  which was close to unity indicated the goodness of the fit and that the experimental values were close to the predicted values. Again, although the  $R^2$  value for  $Y_1$  was lower, its low standard deviation compared with that

of  $Y_2$  showed that the model was still very valid to optimize the experimental parameters. The correlation between the experimental and predicted values of the two models is shown graphically in Fig. 3 for yield and Fig. 4 for percentage removal of AR1 by OPEFB. The proposed models for the two responses percentage yield ( $Y_1$ ) and removal ( $Y_2$ ) are as follows:

$$Y_1 = 18.93 - 4.87x_1 - 0.36x_2 - 1.22x_3 - 2.67x_1^2 - 0.74x_2^2 + 1.87x_3^2 - 2.13x_1x_2 - 0.47x_1x_3 + 2.06x_2x_3$$

5

$$Y_2 = 67.96 + 11.65x_1 + 0.96x_2 + 7.07x_3 + 2.78x_1^2 - 5.11x_2^2 - 0.097x_3^2 + 2.52x_1x_2 + 1.10x_1x_3 + 2.33x_2x_3$$

6

**Table 3** Experimental design matrix for preparation of OPEFB activated carbons

Run	Level			Activated carbon preparation variable			Activated carbon yield, $Y_2$ (%)	RR1 dye removal, $Y_2$ (%)
				Activation temperature, $x_1$ (°C)	Activation time, $x_2$ (min)	Impregnation ratio IR, $x_3$		
1	-1	-1	-1	690.54	84.32	0.91	25.12	50.23
2	1	-1	-1	809.46	84.32	0.91	19.47	69.78
3	-1	1	-1	690.54	155.68	0.91	22.57	45.98
4	1	1	-1	809.46	155.68	0.91	7.9	70.89
5	-1	-1	1	690.54	84.32	2.09	18.68	59.09
6	1	-1	1	809.46	84.32	2.09	10.65	78.32
7	-1	1	1	690.54	155.68	2.09	23.85	59.45
8	1	1	1	809.46	155.68	2.09	7.84	93.46
9	-1.682	0	0	650.00	120.00	1.50	18.51	57.04
10	1.682	0	0	850.00	120.00	1.50	5.34	93.57
11	0	-1.682	0	750.00	60.00	1.50	15.36	52.74
12	0	1.682	0	750.00	180.00	1.50	19.41	53.22
13	0	0	-1.682	750.00	120.00	0.50	25.53	54.35
14	0	0	1.682	750.00	120.00	2.50	24.01	79.98
15	0	0	0	750.00	120.00	1.50	17.52	66.74
16	0	0	0	750.00	120.00	1.50	20.93	68.39
17	0	0	0	750.00	120.00	1.50	18.78	68.56
18	0	0	0	750.00	120.00	1.50	17.76	77.35
19	0	0	0	750.00	120.00	1.50	18.87	58.89
20	0	0	0	750.00	120.00	1.50	19.54	68.01

**Table 4** Model validation of the two responses percentage yield and removal

Model desirability	Activation temperature, $x_1$ (°C)	Impregnation ratio, $x_2$	Activation time, $x_3$ (min)	Activated carbon yield (%)			RR1 removal (%)		
				Predicted	Experimental	Error (%)	predicted	Experimental	Error (%)
	820	2.5	140	19.52	19.12	2.05	96.89	98.81	1.98

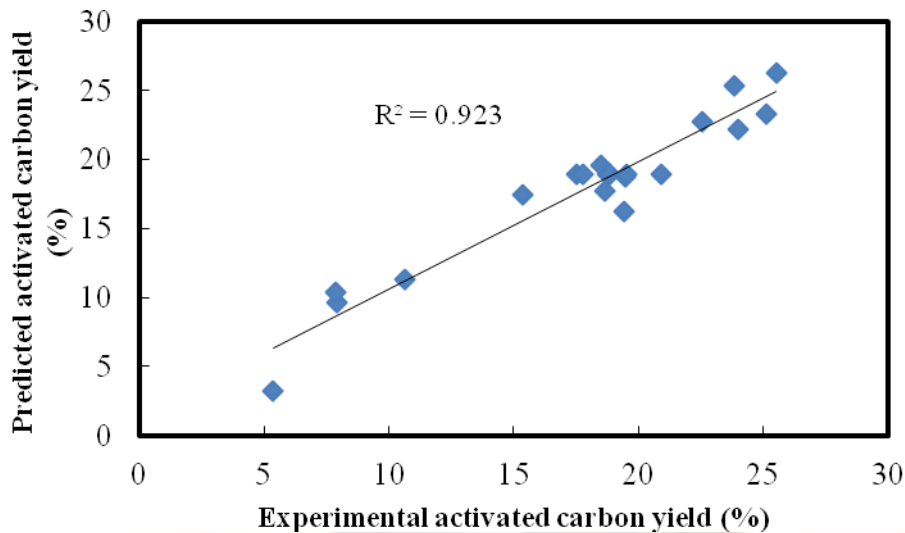


Figure 3 Correlation between the experimental and predicted values for the yield of OPEFB

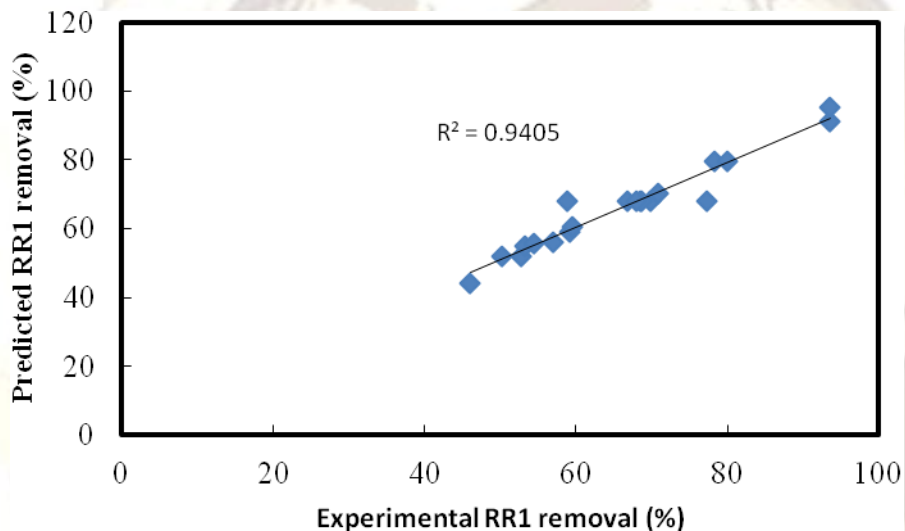


Figure 4 Correlation between the experimental and predicted values for the removal of AR1 with OPEFB activated carbon

### 3.3 The analysis of variance

Analysis of variance ANOVA was used to justify the adequacy and significance of the models through the Fisher's F-test and the probability values. The fisher's variance ratio  $F\text{-value} = (S_r^2/S_e^2)$  is the ratio of the mean square owing to regression to the mean square owing to error; It is the measure of variation in the data about the mean. If values of "Prob > F" less than 0.0500 indicate model terms are significant and greater than 0.1000 indicate the model terms are not significant.

The percentage yield model had  $x_1, x_1^2, x_3^2, x_1 x_2$  and  $x_2 x_3$  as its significant terms and F-value of 13.46 implying that the model is significant; there is only a 0.02% chance that a "Model F-Value" this large could occur due to noise. The details of ANOVA result for the percentage model yield is presented in Table 5.

Table 5 ANOVA for response surface quadratic model for OPEFB activated carbon yield

Source	Sum of squares	Degree of freedom	Mean square	F value	Prob>F
Model	593.36	9	65.93	13.46	0.0002
$x_1$	323.90	1	323.90	66.14	< 0.0001
$x_2$	1.79	1	1.9	0.37	0.5586

$x_3$	20.17	1	20.17	4.12	0.0699
$x_1^2$	102.69	1	102.69	20.97	0.0010
$x_2^2$	7.87	1	7.87	1.61	0.2336
$x_3^2$	50.50	1	50.50	10.31	0.0093
$x_1 x_2$	36.13	1	36.13	7.38	0.0217
$x_1 x_3$	1.73	1	1.73	0.35	0.5655
$x_2 x_3$	33.95	1	33.95	6.93	0.0250
Residual	48.97	10	4.90	-	-

The percentage removal model significant terms were  $x_1$ ,  $x_3$ ,  $x_1^2$  and  $x_2^2$  and it also had F-value of 17.55 implying that the model is significant and that there is only a 0.01% chance that a "Model F-Value" this large could occur due to noise. The result can be found in Table 6. The "Adeq Precision" measures the signal to noise ratio and a ratio greater than 4 is desirable. For the two models percentage yield and removal, the ratio of 14.749 and 16.182 respectively were obtained indicating an adequate signals. These models can be used to navigate the design space.

**Table 6** ANOVA for response surface quadratic model for OPEFB activated carbon removal

Source	Sum of squares	Degree of freedom	Mean square	F value	Prob>F
Model	3187.51	9	354.17	17.55	0.0001
$x_1$	1854.32	1	1854.32	91.90	< 0.0001
$x_2$	12.70	1	12.70	0.63	0.4461
$x_3$	682.50	1	682.50	33.82	0.0002
$x_1^2$	111.45	1	111.45	5.52	0.0406
$x_2^2$	376.64	1	376.64	18.67	0.0015
$x_3^2$	0.14	1	0.14	0.0037	0.9362
$x_1 x_2$	50.70	1	50.70	2.51	0.1440
$x_1 x_3$	9.64	1	9.64	0.48	0.5053
$x_2 x_3$	43.43	1	43.43	2.15	0.1731
Residual	201.78	10	20.18	-	-

### 3.4 The OPEFB activated carbon yield

Activation temperature  $x_1$ , activation time  $x_2$  and chemical impregnation ratio  $x_3$ , were the three parameters studied and they all had impact on the yield of OPEFB activated carbon. The F-values shown in Table 5 revealed that temperature had the greatest impact on the yield while the activation time had the least effect going by the high and low values of the two parameters respectively. It was found that the yield reduced with corresponding increase in temperature which could be attributed to dehydration and elimination reaction. Also, intercalation of potassium hydroxide (activating agent) and loss of carbon in form of carbon dioxide and carbon monoxide which occurs at elevated temperature contributed to the reduction of the yield. The increase in IR was also found to reduce the yield. This was probably due to presence of adequate potassium metal ions for intercalation at elevated temperature. The interaction effects of the parameters also showed significant impact on the yield. This result is similar to the one reported by Ahmad et al [16] and, Lua and Yang [17]. The three dimensional graphs of the interaction effect of the parameters on the yield are shown in Fig. 5a and 5b. The Fig. 5a represents the interaction of activation temperature and impregnation with time fixed at zero level (120 min); while the Fig. 5b had impregnation ratio fixed at zero level (IR=1.5) at the interaction of activation temperature and activation time.

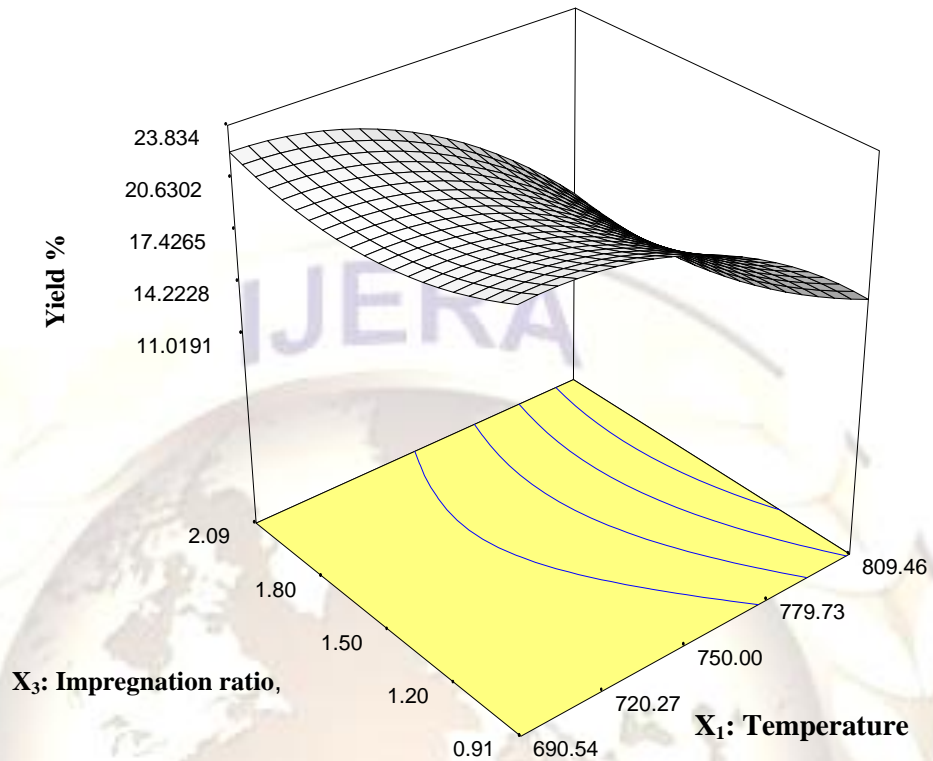


Figure 5a



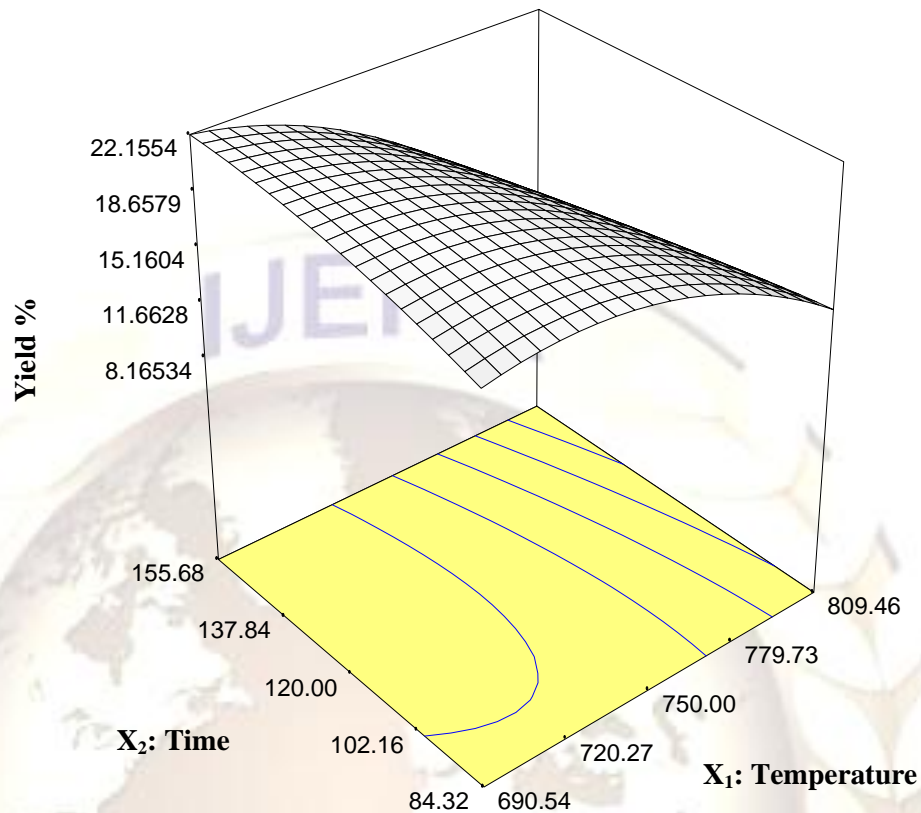


Figure 5b

Figure 5 Three dimensional response surface plot of OPEFB activated carbon yield: (a) effect of activation temperature and IR,  $t=120$  min; (b) effect of activation temperature and time,  $IR=1.5$

### 3.5 Removal of AR1 by OPEFB activated carbon

Table 6 shows the ANOVA result for AR1 removal. It revealed that the greatest significant effect on AR1 removal by OPEFB activated carbon was from activation temperature  $x_1$  of the system, having the highest F-value. Activation time had the least effect while the impregnation ratio of chemical had moderate impact on the removal. It has been reported that unnecessary extension of activation time may lead to enlargement of pores which may not be required, although this depend on the targetted activated carbon application [18]. As mentioned earlier, high temperature and impregnation ratio are required for intercalation of potassium metals and loss of carbon. These activities enhanced the development of pores of the OPEFB activated carbon which reflected on the increased adsorption capacity of the AR1. The result was in agreement with literature that intercalation of potassium metal during activation of carbon with potassium hydroxide is more rapid as from temperatures of  $700\text{ }^{\circ}\text{C}$  and this process promotes development of more pores on the surface of the carbon [19,20]. Although, excess concentration of potassium hydroxide as activation agent may instead of providing more metal for development of pores, lead to formation of intermediates like  $\text{K}_2\text{CO}_3$  which blocks the pores of the activated carbon. This phenomenon leaves the activated carbon with some pores occupied by this compound and consequently reduce the surface area and available pores on the surface [21]. The three dimensional graph of impregnation ratio and temperature parameters with time fixed at zero level ( $t=120$  min) for the percentage removal is shown in Fig. 6.

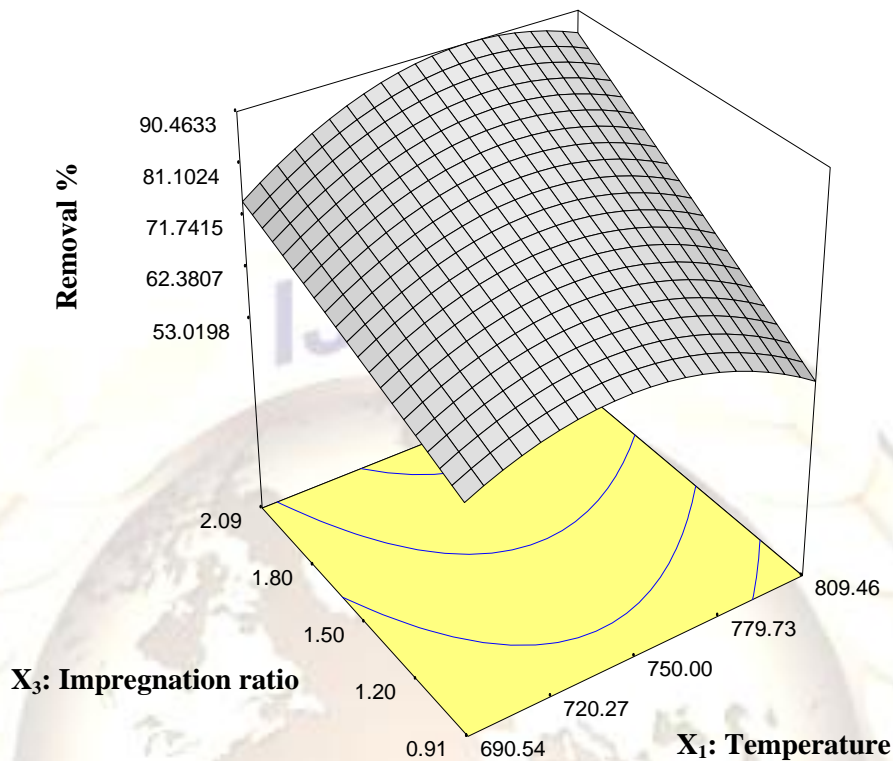


Figure 6 Three-dimensional response surface plot of AR1 percentage removal of OPEFB activated carbons: effect of activation temperature and IR,  $t = 120$  min

#### 4. Conclusion

Activation temperature, activation time and chemical impregnation ratio were adequately optimized as preparation parameters for the two responses: percentage yield of OPEFB activated carbon and percentage removal of AR1 by the carbon produced. The OPEFB activated carbon produced had a surface area of  $820 \text{ m}^2/\text{g}$  and was mesoporous in nature ( $D_p=2.56 \text{ nm}$ ). Activation temperature was found to have greatest significant impact on the two responses percentage yield and removal; while the least effect came from the activation time for the responses targeted. The optimal conditions for the preparation of OPEFB activated carbon for high yield and excellent removal of AR1 were at  $820^\circ\text{C}$ , 140 min and 2.5:1 (ratio of activating agent to precursor) representing the activation temperature, activation time and impregnation ratio, respectively. The results of this study shows that remediation of AR 1 pollutant from waste waters can be effectively carried out with the aid of activated carbon adsorbent produced from OPBEF.

#### References

- [1] E.N. El Qada, S.J. Allen, and G.M. Walker, Adsorption of Methylene Blue onto activated carbon produced from steam activated bituminous coal: A study of equilibrium adsorption isotherm, *Chemical Engineering Journal*, 124(1-3), 2006, 103-110.
- [2] M.A. Ahmad, and R. Alrozi, Optimization of preparation conditions for mangosteen peel-based activated carbons for the removal of Remazol Brilliant Blue R using response surface methodology, *Chemical Engineering Journal*, 165(3), 2010, 883-890.
- [3] R. Gong, M. Li, C. Yang, Y. Sun, and J. Chen, Removal of cationic dyes from aqueous solution by adsorption on peanut hull, *Journal of Hazardous Materials*, B121(1-3), 2005, 247-250.
- [4] K.Y. Foo, B.H. Hameed, Decontamination of textile wastewater via  $\text{TiO}_2$ /activated carbon composite materials, *Advances in Colloid and Interface Science*, 159(2), 2010, 130-143.
- [5] G.G. Stavropoulos, and A.A. Zabaniotou, Minimizing activated carbons production cost, *Fuel Processing Technology*, 9 (7-8), 2009, 952-957.

- [6] S. Chowdhury, R. Mishra, P. Saha, and P. Kushwaha, Adsorption thermodynamics, kinetics and isosteric heat of adsorption of malachite green onto chemically modified rice husk, *Desalination*, 265(1-3), 2011, 159-168.
- [7] T. Hsu, Adsorption of an acid dye onto coal fly ash, *Fuel* 87(13-14), 2008, 3040-3045.
- [8] N.K. Amin, Removal of direct blue-106 dye from aqueous solution using new activated carbons developed from pomegranate peel: adsorption equilibrium and kinetics, *Journal of Hazardous Material* 165(1-3), 2009, 52-62.
- [9] S.W. Won, H. Kim, S. Choi, B. Chung, K. Kim, and Y. Yun, Performance, kinetics and equilibrium in biosorption of anionic dye Reactive Black 5 by the waste biomass of *Corynebacterium glutamicum* as a low-cost biosorbent, *Chemical Engineering Journal*, 121(1), 2006, 37-43.
- [10] M. Auta, and B.H. Hameed, Preparation of waste tea activated carbon using potassium acetate as an activating agent for adsorption of Acid Blue 25 dye, *Chemical Engineering Journal*, 171(2), 2011, 502-509.
- [11] M. Zahangir, S.A. Muyibi, M.F. Mansor, and R. Wahid, Activated carbons derived from oil palm empty-fruit bunches: Application to environmental problems, *Journal of Environmental Sciences*, 19(1), 2007, 103-108 .
- [12] J. Guo, and A.C. Lua, Preparation of activated carbons from oil-palm-stone chars by microwave-induced carbon dioxide activation, *Carbon* 38(14), 2000, 1985-1993.
- [13] J. Diaz-Teran, D.M. Nevskaja, J.L. Fierro, G.A.J. Lopez-Peinado, and A. Jerez, Study of chemical activation process of a lignocellulosic material with KOH by XPS and XRD, *Microporous and Mesoporous Materials*, 60 (1-3), 2003, 173-181.
- [14] B.H. Hameed, I.A.W. Tan, A.L. Ahmad, preparation of oil palm empty fruit bunch based activated carbon for removal of 2,4,6-trichlorophenol: Optimization using response surface methodology, *Journal of Hazardous Materials* 164(2-3), 2009, 1316-1324.
- [15] A. Ozer, G. Gurbuz, A. Calimli, and B.K. Korbahti, Investigation of nickel(II) biosorption on *Enteromorpha prolifera*: optimization using response surface analysis, *Journal of Hazardous Materials*. 152(2), 2008, 778-788.
- [16] A.A. Ahmad, B.H. Hameed, and A.L. Ahmad, Removal of disperse dye from aqueous solution using waste-derived activated carbon: optimization study, *Journal of Hazardous Materials*, 170(2-3), 2009, 612-619.
- [17] A.C. Lua, and T. Yang, Effect of activation temperature on the textural and chemical properties of potassium hydroxide activated carbons, *Journal of Analytical and Applied Pyrolysis*, 76 (1-2), 2004, 96-102.
- [18] M.K.B. Gratuito, T. Panyathanmaporn, R.A. Chumnanklang, N. Sirinuntawittaya, and A. Dutta, Production of activated carbon from coconut shell: optimization using response surface methodology, *Bioresources Technology*, 99(11), 2008, 4887-4895.
- [19] D. Adinata, W.M.A. Wan Daud, and M.K. Aroua, Preparation and characterization of activated carbon from palm shell by chemical activation with  $K_2CO_3$ , *Bioresources Technology*, 98(1), 2007, 145-149.
- [20] I.A.W. Tan, A.L. Ahmad, and B.H. Hameed, Optimization of preparation conditions for activated carbons from coconut husk using response surface methodology, *Chemical Engineering Journal*, 137(3), 2008, 462-470.
- [21] A.N.A. El-Hendawy, An insight into the KOH activation mechanism through the production of microporous activated carbon for the removal of  $Pb^{2+}$  cations, *Applied Surface Science*, 255(6), 2009, 3723-3730.